Published in final edited form as:
*J Immunol*. 2005 January 1; 174(1): 143–154.

# Enhanced Tolerance to Autoimmune Uveitis in CD200-Deficient Mice Correlates with a Pronounced Th2 Switch in Response to Antigen Challenge[1]

**Neil Taylor**[*], **Karen McConnachie**[*], **Claudia Calder**[†], **Rosemary Dawson**[*], **Andrew Dick**[†], **Jonathon D. Sedgwick**[‡], and **Janet Liversidge**[2,*]

[*]Institute of Medical Sciences, University of Aberdeen, Aberdeen, United Kingdom

[†]Division of Ophthalmology, University of Bristol, Bristol, United Kingdom

[‡]DNAX Research, Inc., Palo Alto, CA 94304

## Abstract

A single exposure to inhaled Ag 10 days before immunization leads to long term, Ag-specific tolerance. Respiratory tract myeloid APCs are implicated, but how regulation is invoked, and how tolerance is sustained are unclear. This study examines the in vivo function of the myeloid regulatory molecule CD200 in the process of tolerance induction. Despite earlier onset of experimental autoimmune uveitis in sham-tolerized, CD200-deficient mice, disease incidence and subsequent severity were actually reduced compared with those in wild-type mice. Protection was more effective and long term, lasting at least 28 days. Halting disease progression and tolerance in $CD200^{-/-}$ mice correlated with a marked increase in Th2-associated cytokine production by Ag-challenged splenocytes. Reduced overall disease and enhanced tolerance in the CD200-deficient mice in this model system were unexpected and may be related to altered populations of MHC class $II^{low}$ APC in the respiratory tract compared with wild-type mice together with associated activation of STAT6 in draining lymph nodes of tolerized mice. These data indicate that in the absence of default inhibitory CD200 receptor signaling, alternative, powerful regulatory mechanisms are invoked. This may represent either permissive dominant Th2 activation or an altered hierarchy of negative signaling by other myeloid cell-expressed regulatory molecules.

Regulation of immune responses to infection or injury requires both initiation signals and termination signals to restore and maintain peripheral tolerance and immunologic homeostasis. IL-10 in particular plays a key role in controlling and terminating inflammatory responses (1-3), with fine-tuning of the immune response to Ag challenge being accomplished by gene families encoding related receptors with opposing functions (4). APCs of the myeloid lineage, such as macrophages and dendritic cells (DC),[3] are central to these regulatory processes (5). The importance of this modulation is demonstrated by the sometimes fatal autoimmune and lymphoproliferative disorders observed in mice with targeted disruption of inhibitory receptors for IL-10 signaling (6).

[1]This work was supported by project grants from the Wellcome Trust, Tenovus Scotland, Grampian Universities Hospitals National Health Service Trust Endowments, and the National Eye Center, Bristol. DNAX is supported by Schering Plough Corp. (Kenilworth, NJ).



[2]Address correspondence and reprint requests to Dr. Janet Liversidge, College of Medicine and Medical Sciences, Institute of Medical Sciences, University of Aberdeen, Foresterhill, Aberdeen, U.K. AB25 2ZD. E-mail address: j.liversidge@abdn.ac.uk.

The costs of publication of this article were defrayed in part by the payment of page charges. This article must therefore be hereby marked *advertisement* in accordance with 18 U.S.C. Section 1734 solely to indicate this fact.


Europe PMC Funders Author Manuscripts

In myeloid cells, activating and inhibitory receptor pairs form a family of triggering receptors that include activating triggering receptors expressed by myeloid cells as well as signal-regulating proteins SIRP$\alpha$ and SIRP$\beta$ that have reciprocal roles in myeloid cell function (7-9). Now CD200 (OX-2 Ag) (10, 11) has been identified as a negative regulator of myeloid APCs that might be manipulated to provide therapeutic effects in autoimmunity and transplantation (12-14). CD200 is reported to be expressed by a variety of cells, including neurons and microvascular endothelium, and can be induced by activated T cells (15), whereas strong expression of its structurally related inhibitory receptor (CD200R) is largely restricted to cells of the myeloid lineage, including monocyte macrophages, DC, and microglia (11, 16-18). Recently, additional members of the CD200R family have been identified in mice (19). In addition to the inhibitory CD200R, which is known to be expressed by $CD4^+$ T cells, especially polarized Th2 cells, there are at least two potentially activating isoforms, designated mCD200RLa and mCD200Lb. The latter do not bind to CD200 and have unknown ligands, but, in common with other receptor pairs, they have potential activating function through DNAX-activating protein-12 (DAP-12) adapter protein binding. These receptors also show differential, low levels of expression on other leukocyte subsets, supporting the idea that rather than merely representing redundancy of function, receptor pairs may have specialized functions in specific cells or tissues.

CD200-deficient mice ($CD200^{-/-}$) exhibit various myeloid defects. These include elevated numbers of macrophages within tissues normally expressing CD200 and increased DAP-12 expression, particularly in the marginal zone of secondary lymphoid tissues, indicating myeloid cell activation. As a consequence of this phenotype, mice lacking CD200 appear to have increased susceptibility to CD4 T cell-mediated autoimmune diseases (12). In particular, CD200/CD200R regulation of microglial activation has profound effects on neuronal tissues, accelerating the onset of experimental models of autoimmunity affecting the CNS, including experimental autoimmune encephalomyelitis (EAE) (12) and experimental autoimmune uveoretinitis (EAU) (20).

EAU is mediated by retinal Ag-specific $CD4^+$ T cells and can be modulated using various therapeutic approaches targeting Th cell function (21, 22), including induction of Ag-specific tolerance via the nasal mucosa (23-25). Activated macrophages are also required for full expression of disease (26-29), but, equally, macrophages are required for resolution of inflammation. For instance, macrophages respond to signals such as IL-4 and IL-10 and actively participate in the anti-inflammatory process (30-32), demonstrating that,

[3]Abbreviations used in this paper:

| | |
|---|---|
| DC | dendritic cell |
| BMDC | bone marrow-derived DC |
| DAP-12 | DNAX-activating protein-12 |
| EAE | experimental autoimmune encephalomyelitis |
| EAU | experimental autoimmune uveoretinitis |
| NOS2 | type 2 NO synthase |
| RTDC | respiratory tract DC |
| $T_{reg}$ | regulatory T cell |
| WT | wild type |

alternatively, activated macrophages are important for healing and tissue remodeling. Such alternatively activated macrophages have recently been described by us in the rat model of EAU (33). Myeloid APC may also have a dual role in nasal tolerance induction in EAE and EAU, where signaling by neuronally expressed CD200 must occur during the inflammatory process. In these models effective protection is associated with an initial IFN-$\gamma$-driven priming event in cervical lymph nodes, followed by T cell apoptosis and down-regulation of the capacity of Ag-specific T cells to proliferate in response to restimulation (34, 35). IL-10 has been shown to have a pivotal role in this process (36, 37). How are these contradictory, but complementary, activities of macrophages and DC affected by the CD200/CD200R interaction?

In this study we use a model of tolerance induction by respiratory exposure to Ag in $CD200^{-/-}$ mice to examine the role of CD200/CD200R interactions in vivo on tolerance induction and maintenance. We chose the moderately susceptible C57BL/6 mouse EAU model (38) because uveitogenic T cells alone are insufficient to cause target organ damage. Monocyte macrophages are also necessary and prominent in the earliest inflammatory infiltrates in the retina (26). In addition, monocyte expression of type 2 NO synthase (NOS2) is required for full expression of disease (27, 39, 41). Respiratory tract DC (RTDC) and alveolar macrophages are known to be involved in tolerance induced by respiratory exposure to Ag (37, 41). T cell activation and proliferation in the draining cervical lymph are followed by systemic generation of regulatory cells in the spleen (24, 35, 42), providing a model to study myeloid APC function and T cell regulation in vivo. The data presented show that despite the accelerated disease onset that is expected in the absence of inhibitory CD200R signaling, overall disease incidence and severity were significantly reduced over time in $CD200^{-/-}$ mice. This result was unpredicted, but correlated with elevated numbers of regulatory T cells ($T_{reg}$) and the presence of high IL-10-secreting splenic myeloid cells later in the disease process. Induction of tolerance to retinal Ag was also enhanced in CD200-deficient mice, which demonstrated an altered phenotype of APC in the respiratory tract and an enhanced Th2 switch compared with wild type (WT).

## Materials and Methods

### Animals and induction of EAU

CD200-deficient mice ($CD200^{-/-}$) on the C57BL/6 background were generated at DNAX (Palo Alto, CA), and an isolator-reared, specific pathogen-free breeding colony was established within the biological services unit of Aberdeen University. Specific pathogen-free C57BL/6 wild type ($CD200^{+/+}$) mice were purchased from Harlan Olac. Groups of three to eight mice were used as detailed in the text or figure legends for each experiment. For immunization, groups of sex and age matched mice were used at 6-8 wk of age. Mice were immunized by s.c. injection of 500 $\mu$g of peptide 1-20 of interphotoreceptor retinoid binding protein (Sigma-Genosys) in CFA (2.5 mg/ml *Mycobacterium tuberculosis*) plus 1 $\mu$g/ml *Bordetella pertussis* toxin i.p. as an additional adjuvant (38). At specified times animals were killed by $CO_2$ asphyxiation, and eyes were enucleated for resin histology (H&E staining for histological scoring system) or for immunocytochemistry. Lymphoid tissue was also sampled to determine peptide-specific proliferative and cytokine responses. The severity of disease was assessed using a modified version of our histological grading system for rat EAU. At least three sections from each eye were scored in a masked fashion using a semiquantitative scoring system that combines the extent of the inflammatory infiltrate with tissue damage in the posterior chamber (23). All results are expressed as the mean ± 1 SEM. Comparison of histological assessment of disease in $CD200^{-/-}$ and $CD200^{+/+}$ were analyzed using the Mann-Whitney $U$ test (Instat software; GraphPad), and $p \leq 0.05$ was considered significant. Disease incidence was analyzed using Fisher's exact test, and $p \leq 0.05$ was considered significant.

### Induction of tolerance

Mucosal tolerance was induced by intranasal administration of 50 $\mu$g of peptide in 5 $\mu$l of PBS or 5 $\mu$l of PBS alone using an Oxford pipette. This regimen, administered 10 days before immunization has previously been shown to be effective in modulating EAU (25). In some experiments mice were killed at intervals over the following 48 h to examine the effects of intranasal peptide on cells in draining cervical lymph nodes and spleens or in control submandibular and mesenteric lymph nodes. In other experiments animals were immunized 10 days later with peptide or PBS in CFA with *B. pertussis* toxin.

### Proliferation and cytokine profile assays

Lymphocyte proliferative responses to recall Ag were measured using the BrdU Flow kit (BD Biosciences) according to the manufacturer's instructions. This test has the advantage of more detailed analysis of viable cell cycle kinetics by combining BrdU labeling of cells in S phase with measurement of total DNA content of the population as a whole. Single-cell suspensions were obtained from individual spleens by pressing the tissue through a 250-$\mu$m pore size metal sieve, and mononuclear cells were purified by Percoll density gradient centrifugation. RBC were removed by hypotonic lysis. Cultures were set up at a density of $1 \times 10^6$ cells/ml with 10 $\mu$g/ml peptide 1-20 for 96 h. This time period was established as optimum by compiling data from 48- to 120-h incubations in preliminary experiments. Each well was then pulsed with 10 $\mu$l of 1 mM BrdU for 45 min and harvested, and cells were permeabilized with Cytofix/Cytoperm (BD Biosciences) and frozen at -80°C in FCS with 10% DMSO (Sigma-Genosys) before staining and analysis. An FITC-labeled anti-BrdU Ab was used to identify the extent of BrdU incorporation, and the DNA stain 7-aminoactinomycin D was used to quantify the total DNA content. Measurements were made by two-color flow cytometry using a FACSCalibur or a FACS LSR (both from BD Biosciences, Mountain View, CA) with flow rate adjusted to give the optimal coefficient of variation of the DNA peaks. Data were obtained from at least three individual animals at each time point. Results were expressed as the mean ± SEM. For cytokine profile analysis of responding cultures, parallel 1-ml cultures were set up with $4 \times 10^6$ cells and 10 $\mu$g/ml peptide. After 72 h, supernatants were harvested, clarified by centrifugation, aliquoted, and frozen at -30°C until assay. Negative control cultures contained PBS in place of peptide, and 2.5 $\mu$g/ml Con A was added to positive control cultures to demonstrate optimum growth conditions.

IL-10 and IL-12 were measured using optELISA kits (BD Pharmingen) exactly according to the manufacturer's instructions. The mouse cytokine bead array (CBA kit; BD Pharmingen) was used to measure other cytokines. Results are expressed as the mean ± SEM of supernatants from at least six animals in each group, and differences were considered significant at a value of $p < 0.05$ using unpaired Student's $t$ test.

### Isolation and phenotyping of respiratory tract cells

Mice were anesthetized with 0.1 ml of Sagatol (Aventis Pharma) i.p. and were perfused with $Ca^{2+}/Mg^{2+}$-free PBS containing 10 U/ml heparin and 5 mM EDTA to remove blood from the respiratory tract vessels. The lungs and trachea were removed and disrupted mechanically by chopping and passing through a 250-$\mu$m pore size mesh. The resulting suspension was collected and treated with 0.7 mg/ml collagenase and 30 U/ml DNase in RPMI 1640 for 1 h at 37°C with agitation. The cells were then washed and passed through a 100-$\mu$m pore size mesh before centrifugation over Percoll 1.075. Cells were then washed, and $CD45^+$ cells were analyzed by flow cytometry (FACSCalibur) for myeloid phenotype (CD11b, CD11c, F4/80, and CD204) and for activation markers (MHC class II, CD40, CD80, and CD86) as described below.

To determine myeloid cell distribution within the tissue, cryostat sections of Evan's Blue-perfused lung tissue were stained with FITC-conjugated CD11b mAb M1/70 or IgG control mAb R35-95 (BD Pharmingen), and digital images were captured with an LSM confocal microscope (Zeiss) using the same laser settings for each image in the experiment. The relative abundance of CD11b fluorescence signal in each image was analyzed by measuring pixel values within defined regions using Laserpix software (Bio-Rad). Positively staining cells were counted using the Count-Size command and the Histogram command used to measure the average intensity value (mean) of positively stained cells.

### Generation of bone marrow-derived DC (BMDC)

BMDC were prepared by a modification of the procedure described by Inaba et al. (43) as previously described (44). Briefly, $7.5 \times 10^5$ precursors were set up in 1-ml cultures supplemented with GM-CSF. The cultures were fed, and nonadherent cells were removed every 2 days by swirling and aspirating 75% of medium and adding fresh growth medium with GM-CSF. Developing DC remained attached to the bed of firmly adherent macrophages. Six days after initiation of the cultures, the loosely adherent clusters of DC were harvested, and contaminating granulocytes were depleted using anti-mouse Gr-1 mAb (RB6-8C5; BD Pharmingen) and Dynabeads (Dynal Biotech). Purified BMDC were further seeded at $1 \times 10^6$/ml/well in 24-well plates supplemented with GM-CSF. Then 1 $\mu$g of LPS was added to the cultures at various time points (0-24 h). Supernatant was then collected from each well 22 h after administration of LPS for cytokine measurement. Medium alone DCs were used as control.

### Immunocytochemistry

Eyes from immunized mice or lymphoid tissue were dissected, snap-frozen in OCT (Miles), and 7-$\mu$m serial sections were cut, air-dried, and fixed in 100% cold acetone for immunocytochemistry using the alkaline phosphatase anti-alkaline phosphatase technique. After rehydration in TBS, sections were blocked with TBS/1% normal rabbit serum and then avidin D block solution (Vector Laboratories) for staining with polyclonal rabbit anti-STAT 4 (C20; Santa Cruz Biotechnology) STAT 6 (M20; Santa Cruz Biotechnology) or with phosphorylated STAT6 (Tyr641; New England Biolabs) using irrelevant polyclonal Ab and blocking peptides as negative controls. Other sections were stained using rat mAbs to murine CD3 and myeloid cell markers F4/80 Ag (CI:A3-1), MOMA-1, and MOMA-2 (Serotec). Activation markers included NOS2 (clone 6; Transduction Laboratories), rat anti-mouse CD86 (GL-1; BD Pharmingen), and MHC class II (I-Ab; P7.7; Serotec). Positive staining was detected by mouse absorbed biotinylated anti-rabbit Ig-alkaline phosphatase or biotinylated anti-rat Ig-alkaline phosphatase conjugate, followed by streptavidin:avidinbiotin peroxidase-alkaline phosphatase complex and Fast Red substrate (DakoCytomation) lightly counterstained with hematoxylin. Sections for image analysis were cut and stained in batches to ensure uniform labeling conditions for each Ab. Sections were then analyzed using the Aphelion Active X image analysis program from ADCIS. The program was adapted using Visual basic to allow analysis of immunostaining in user-defined regions of the image. An average value (percentage of tissue stained per ×20 field) for each section was obtained from four to six fields. Results are expressed as the mean ± SEM of tissue from a minimum of three animals per treatment group. Differences between groups were analyzed using unpaired Student's $t$ test, and $p < 0.05$ was considered significant.

### Flow cytometry

A FACSCalibur or FACS LSR (BD Biosciences) was used for data acquisition, and CellQuest software (BD Biosciences) was used for data analysis. APCs and lymphocytes isolated from lymph nodes and spleens were evaluated by multicolor immunofluorescent staining with mAbs to the following cell surface markers: CD11b (M1/70), CD11c (HL3),

CD4 (RM4-4) CD45RB (16A), CD45R/B220 (RA3-6B2), CD40 (3/23), CD86 (GL-1), CD152 (BN13), MHC class II (I-Ab; AF6-120.1), CD25 (PC61), CD38 (92), CD8a (53-6B2), CD62L (MEL-14), and CD3$\epsilon$ (145-2C11) were all from BD Pharmingen. For intracellular detection of IL-10, quadruple staining was performed. Cells were treated with Cytofix-Cytoperm and stained with PE-conjugated anti-IL-10 (JES5-16E3) following the manufacturer's instructions (BD Pharmingen). Anti-CD204 (2F8), F4/80 (CI:A3-1), metallophillic macrophages (MOMA-1), and CD80 (RMMP-1) were obtained from Serotec. These were conjugated to FITC, PE, allophycocyanin, PerCP, PerCP-Cy5.5, or biotin as required. Biotin-labeled Abs were detected by addition of streptavidin-allophycocyanin (1/400; BD Pharmingen). Negative isotype controls and single positive controls were performed to allow accurate breakthrough compensation. Gates and instrument settings were set according to forward and side scatter characteristics, and populations were gated to exclude dead or clumped cells. A total of 10,000 events were collected. Fluorescence analysis was performed after additional backgating to exclude nonspecific or background staining. Data were collected from at least four individual animals at each time point in each experiment; the cells were prepared and stained for analysis on the same day. Histogram results are expressed as the mean ± SEM. Results shown are representative of at least four separate experiments.

### Immunoprecipitation of STAT6

Activation of STAT6 expression was also demonstrated by immunoblotting of immunoprecipitates prepared from cytosolic and nuclear extracts from lymphoid tissues as previously described (43). Briefly, cytosolic extracts were prepared from 10 (7, 8) cells in 20 $\mu$l of lysis buffer A. Nuclei were removed by centrifugation, and supernatants were clarified and collected as the cytoplasmic fractions. Nuclei were then incubated in 20 $\mu$l of lysis buffer B (containing 0.42 M NaCl) and centrifuged, and supernatants were collected as nucleic fractions. STAT6-associated proteins were immunoprecipitated by anti-STAT6 Ab (M20; Santa Cruz Biotechnology), collected on protein A-Sepharose beads (Amersham Biosciences, Arlington Heights, IL), and resolved by SDS-PAGE. Protein was transferred onto a Hybond polyvinylidene difluoride membrane (Amersham Biosciences) by electroblotting. Initial probing was performed for phosphotyrosine (mAb 4G10; Upstate Biotechnology) detected by ECL. Membranes were then stripped and reprobed with STAT6 Ab to confirm the specificity of the signal.

## Results

### Tolerance induction in CD200$^{-/-}$ mice is robust, and disease incidence and severity are significantly reduced compared with those in WT mice

Mice were given either peptide 1-20 (tolerized group) or control PBS (sham-tolerized group) intranasally 10 days before immunization. Fig. 1 shows the pattern of disease progression in tolerized and control WT and CD200$^{-/-}$ mice over time. In WT mice, disease progressed rapidly, with all mice showing moderate to severe retinal inflammation and photoreceptor damage by 21 days postimmunization, persisting to day 28. In accordance with our previous observations (20), disease onset was accelerated in sham-tolerized CD200$^{-/-}$ mice, with expression of NOS2 in cells of the ciliary body, retinal vascular endothelium, and inner plexiform layer (IPL) of the retina being the earliest signs of disease on day 10 (Fig. 2, *a* and *b*) and significantly elevated disease scores by day 16 ($p < 0.03$). However, as in our previous study, no overall increase in tissue damage compared with WT mice was observed, and no additional significant disease progression occurred in sham-tolerized CD200$^{-/-}$ mice. By day 28 postimmunization, disease scores were, in fact, significantly lower than those in sham-tolerized WT mice ($p < 0.05$), with 17% mice still showing no signs of disease. No significant increase in histological scores of either sham-tolerized or tolerized CD200$^{-/-}$

mice from days 16-28 postimmunization was found. Significant reductions in the overall histological scores in both tolerized groups compared with their sham-tolerized controls were also observed on day 16 (WT, $p < 0.01$; $CD200^{-/-}$, $p < 0.03$; Fig. 2, *c-f*). No significant difference in overall histological scores between tolerized WT and tolerized $CD200^{-/-}$ mice were found, but on day16, disease incidence in tolerized $CD200^{-/-}$ mice was significantly higher than that in WT tolerized mice ($p < 0.05$), reflecting an earlier onset of disease in these mice. By day 28, however, the situation was reversed, and disease incidence in the $CD200^{-/-}$ tolerized group was very significantly reduced compared with that in tolerized WT mice ($p < 0.006$) as disease incidence continued to increase in the WT groups.

Despite severe disease in WT mice, protection was maintained in the tolerized groups at all time points ($p < 0.01$). In the tolerized $CD200^{-/-}$ group, protection was also effective. Disease scores were significantly reduced on day 16 ($p < 0.03$) and day 28 ($p<0.01$), with up to 50% of the animals still showing no signs of disease.

## In vitro proliferation of splenocytes does not correlate closely with in vivo inflammation during early disease, but is reduced in tolerized mice in late disease

In a previous study we showed that T cell proliferative responses by splenocytes to immunizing peptide 1-20 were equivalent in both WT and $CD200^{-/-}$ mice (20). We confirmed this result using a sensitive flow cytometric assay that combines BrdU labeling of cells in S phase with measurement of total DNA content of the population as a whole (Fig. 3*a*). It was also found that intranasal exposure to Ag had no inhibitory effect on peak proliferation of splenocytes on day 16 or day 21 despite evidence of a significant reduction in disease in tolerized animals at these time points (Fig. 1); however, proliferation by splenocytes from $CD200^{-/-}$ tolerized mice was significantly reduced compared with that in tolerized WT mice ($p < 0.02$). By day 28 postimmunization, the numbers of cells in S phase were reduced in both tolerized groups, and this was highly significant in the $CD200^{-/-}$ tolerized group compared with the sham-tolerized group ($p < 0.01$). Analysis of DNA content of cells suggested that this reduction of cells in S phase was due to reduced turnover of proliferating cells rather than a block in cell cycle progression or an increase in apoptotic or necrotic cells within the cultures (Fig. 3, *b-d*).

## Protection from disease in $CD200^{-/-}$ mice correlates with a switch to IL-4 and IL-5, followed by IL-10 production by restimulated splenocytes

Splenocyte cultures set up in parallel with the proliferation assays were analyzed for cytokine production in response to restimulation with peptide (Fig. 4). Significantly higher levels of IL-4 were found in the tolerized $CD200^{-/-}$ groups on days 16 and 21 ($p < 0.02$, and $p < 0.04$ compared with sham-tolerized $CD200^{-/-}$ mice; $p<0.01$ compared with tolerized WT mice at the same time point). IL-5 was also elevated in $CD200^{-/-}$ tolerized mice on day 21 ($p < 0.04$ compared with sham-tolerized $CD200^{-/-}$; $p<0.02$ compared with tolerized WT). This pattern was replaced by enhanced levels of IL-10 in the $CD200^{-/-}$ tolerized mice by day 28 ($p < 0.05$ compared with sham-tolerized; $p < 0.02$ compared with WT tolerized). IL-2 and TNF were elevated in sham-tolerized WT mice on days 16 and 21 and were significantly reduced in tolerized WT on day 16 ($p < 0.05$). Levels of IL-12 were low in all the cultures. Large quantities of IFN-$\gamma$ (5-15 ng/ml) were also generated in all the cultures at all time points, but no significant differences between groups were observed (data not shown). Changes in IgG2a/IgG1 ratios can be indicative of changes in the Th1/Th2 balance of an immune response. However, due to the short half-life of mouse Ig isotypes (6-8 days for both IgG1 and IgG2a), these were inconclusive given the time span of these experiments (2-4 wk; data not shown).

### STAT-6 is up-regulated in draining lymph nodes and spleen of CD200 deficient mice

The cytokine secretion assays indicated that tolerance in the CD200$^{-/-}$ mice appeared to be accompanied by an earlier and more pronounced Th2 switch in response to restimulation by Ag. To test whether this represented a different response to the tolerization regimen in CD200$^{-/-}$ mice we examined the effect of intranasal administration of Ag on cells of the draining lymph nodes and spleen. Expression of phenotypic myeloid cell markers, MHC class II, APC costimulatory molecules CD80 and CD86 as well as STAT 4 and STAT 6 were measured by image analysis of serial sections of immunostained tissue. Cervical lymph nodes that drain the nasal mucosa, lymphoid areas (white pulp) and macrophage areas (red pulp) of the spleen were examined up to 48 h post intranasal application of Ag. The submandibular lymph nodes were analyzed in parallel to serve as control tissue. Fig. 5, *a-d*, and Table I show that STAT6, which controls the Th2 differentiation pathway (45, 46), was markedly up-regulated in the spleen and cervical lymph nodes of tolerized CD200$^{-/-}$ mice 24 h after treatment. The effect was transient in the cervical nodes, levels returning to control levels by 48 h, but sustained in both lymphoid and macrophage areas of the spleen. Expression of STAT6 was also increased in the spleens, but not lymph nodes of WT mice, where levels actually declined. Immunostaining of sections with an Ab to phosphorylated STAT6 showed activation of the STAT6 pathway in the cervical lymph nodes (Fig. 5, *e* and *f*), and this was confirmed by Western blotting of cytosolic and nuclear extracts, which showed translocation of STAT6 from cytosol to nucleus in CD200$^{-/-}$, but not WT spleens (Fig. 5, *g* and *h*). STAT4, which is activated after IL-12 signaling to drive Th1 responses (47, 48), was also transiently increased in draining lymph nodes and spleen of CD200$^{-/-}$ mice 24 h post-treatment (Table I). This was consistent with the initial Th1 priming previously observed in our rat tolerance model (24) and was accompanied by increased CD86 expression in cervical lymph nodes. However, in contrast, no increase in STAT4 expression was observed in the WT mice, levels actually falling during the sampling period. It was noted that overall expression STAT4 was low compared with STAT6 in this strain of mouse and may be consistent with the low levels of IL-12 p70 generated by Ag-restimulated splenocytes (Fig. 4).

With the exception of a significant increase in STAT6, and a transient increase in STAT4 expression in CD200$^{-/-}$ mice, no significant differences between control and test tissues were observed in the control submandibular tissue. Compared with percentages for cervical tissue, increases were comparatively small. This might reflect changes induced locally through ingestion of very small quantities of Ag during intranasal administration, the effects of disseminated Ag (24), or the systemic effects of changes in the spleen in these animals. No substantial or consistent changes in the percentage of F4/80- or MOMA-2-positive cells after treatment or between groups was observed to account for increased or decreased STAT expression in the tissues. Similarly, although some fluctuation in MHC class II expression was apparent, no significant pattern was found (data not shown).

### DC from CD200$^{-/-}$ mice do not have a defect in IL-12 production

Low production of IL-12 in the Ag-restimulated spleen cells (Fig. 4) together with the low levels of STAT4 Ag detected in the lymph nodes and spleens (Table I) may represent a fundamental deficiency in CD200$^{-/-}$ mice that reduced their ability to mount a normal Th1 response, allowing a Th2 response to emerge by default. To determine the IL-12 vs IL-10 secretion potential of APC from CD200$^{-/-}$ mice, we used the model developed by Jiang et al. (44) that allows BMDC to be matured to secrete either IL-10 or IL-12. BMDC from WT C57BL/6 and CD200$^{-/-}$ C57BL/6 mice secreted both IL-10 and IL12 at high levels (>700 pg/ml) and with similar kinetics, indicating that there was no fundamental defect in the mice to account for the low IL-12 responses observed in our model (data not shown).

### Altered phenotype of respiratory tract APC in CD200$^{-/-}$ compared with WT mice

RTDC have been shown to preferentially stimulate Th2 responses (41) and are implicated in the induction of tolerance to nasally administered Ags (37). Because altered populations of myeloid cells are a major feature of CD200$^{-/-}$ mice (12), we compared the phenotype of CD45$^+$ cells from the respiratory tracts of WT and CD200$^{-/-}$ mice isolated and purified using collagenase/DNase digestion and density gradient centrifugation. In WT mice, the major population isolated were CD11c$^+$ DC (<80%), with few (10-15%) CD11b$^+$ cells. In contrast, in CD200$^{-/-}$ mice, CD11b$^+$ cells formed a far larger proportion (<40%) of the purified cell population, with fewer CD11c$^+$ DC (35-40%; Fig. 6*a*). The cells from both WT and CD200$^{-/-}$ exhibited low levels of activation markers, as expected for respiratory tract APC, but it was also apparent that both CD11b$^+$ and CD11c$^+$ cells from CD200$^{-/-}$ respiratory tract expressed lower levels of MHC class II Ag than WT (Fig. 6*b*). Confocal analysis of respiratory tract tissue showed that this increased proportion of CD11b$^+$ cells present in CD200$^{-/-}$ mice was, in fact, due to increased numbers of CD11b$^+$ cells within the tissue ($p < 0.001$; Fig. 6*c*). Increased detection was not due to higher levels of CD11b expression by positively stained cells, because there was no difference in average pixel intensity between the groups (Fig. 6*d*).

### CD25$^+$ T$_{reg}$ and IL-10$^{high}$ APC are present in the spleens of tolerized CD200$^{-/-}$ mice

Tolerance induced by respiratory tract exposure to Ag has been shown to be dependent on IL-10 and may be mediated by T$_{reg}$ (3, 36, 37). Regulatory cells are also known to be induced by an increase in Ag-specific Th2 activity together with decreased CNS infiltration in a C57BL/6 mouse model of EAE (49). We therefore used flow cytometry to examine the spleens of tolerized, immunized mice for the presence of T$_{reg}$ cells and to identify the phenotype of IL-10-secreting cells. Permeabilization of cells to detect intracellular Ag can reduce or interfere with the fluorescence of surface markers such as CD25, so we used triple fluorescence on unpermeabilized cells to establish the numbers of CD3$^+$CD4$^+$CD25$^+$ present in the spleens of control and treated mice (Fig. 7*a*). In unimmunized control mice, ~5-8% of CD3$^+$ T cells from the spleen displayed the CD3$^+$CD4$^+$CD25$^+$ (contact-dependent) regulatory cell phenotype (data not shown). This was typically increased to 10-15% in immunized mice. A trend toward higher numbers of CD4$^+$CD25$^+$ cells in the CD3$^+$ gated population in CD200$^{-/-}$ mice was noticed, and the number was significantly elevated in tolerized CD200$^{-/-}$ mice compared with tolerized WT mice at all time points (day 16, $p<0.01$; days 21 and 28, $p < 0.05$). All CD3$^+$CD4$^+$CD25$^+$ cells were also CTLA-4$^+$ (data not shown).

IL-10 may be produced by CD25$^+$ T$_{reg}$ cells (50), but Fig. 7*b* shows that CD3$^+$ T cells did not express levels of intracellular IL-10 above background. IL-10-producing cells were found within the spleen myeloid cell population. Two main populations could be identified from day 21 onward. These were predominantly IL-10$^{low}$CD11b$^+$ or small numbers of IL-10$^{high}$CD11c$^{low/-}$ (Fig. 7*b*). IL-10$^{low}$-secreting CD11b$^+$ were also observed at later time points (day 28) in all mice (data not shown), but no significant differences between the groups were found.

It should be noted that the levels of IL-10 detected in these cells should reflect the in vivo situation, because cells were isolated and analyzed directly ex vivo. The cells were not given additional activation stimuli, and Golgi function was not blocked to artificially increase intracellular cytokine levels.

## Discussion

In this study we have examined the role of CD200, an inhibitory ligand for myeloid cells, in a model of tolerance induction to a retinal autoantigen. Unexpectedly, we found that although disease onset in $CD200^{-/-}$ mice was accelerated, in agreement with previous studies using these mice (12, 20), over the longer term, overall disease incidence and severity compared with WT were significantly reduced. Furthermore, tolerance induction in $CD200^{-/-}$ was efficient, with up to 50% of eyes still protected from disease 28 days postimmunization (Fig. 1). Given our current understanding of the CD200/CD200R axis (15, 17, 20) and the results of other studies showing enhanced immunosuppression in autoimmune or transplant models where CD200 expression is elevated or signaling is potentiated by infusion of CD200 immunoadhesions (14, 51), these findings are counterintuitive.

Protection in tolerized $CD200^{-/-}$ mice appeared to correlate with increased Th2-associated cytokines and IL-10 in response to recall Ag, and overall reduced disease in sham-tolerized $CD200^{-/-}$ mice may be associated with the emergence of IL-10-secreting cells in the spleen later in the disease process. Based on the apparent redundancy in regulatory mechanisms controlling potentially tissue damaging inflammation, one possibility is that in a normal individual, the CD200/CD200R axis alone is not critical for the maintenance of immunological homeostasis (although it may contribute to it), but during inflammation, in the absence of default and necessary CD200/CD200R signaling, other regulatory mechanisms are invoked to convert the classically activated myeloid phenotype to an alternatively activated, healing, and immunomodulatory phenotype.

In support of this hypothesis is the emerging principle of dominant inhibitory signaling mediated by self-receptors that governs the maintenance of self-tolerance. Triggering receptors expressed by tissue-trafficking APC such as macrophages and DC or other leukocytes are key molecules in this process (4, 52, 53). In addition to these myeloid cell receptors, active self-regulation to control autoreactive T cell expansion through naturally occurring $CD4^+CD25^+$ T cell populations is now well accepted (54, 55). These, together with induced regulatory mechanisms driving pathogen-specific Th1/Th2 responses through differential cytokine expression (reviewed by in Ref. 56), induction of type 1 $T_{reg}$ cells (reviewed in Ref. 57), and alternative macrophage activation and scavenger receptor expression (29, 58) are invoked to avoid excessive immune pathology. How these diverse regulatory mechanisms interact in complex in vivo models, and the rules governing functional redundancy and hierarchy of responses have yet to be fully understood.

Recently, it has been shown that the CD200R gene family also has receptor isoforms with potential inhibitory and activating functions (19). In addition to the inhibitory isoform that binds CD200 and regulates myeloid activity in the mouse, at least two activating isoforms (CD200RLa and CD200RLb) were identified. These isoforms probably have alternative ligands and are able to pair with the adaptor protein DAP-12, supporting the idea that the CD200R family is also involved in fine-tuning of myeloid cell responses (15). Pertinent to the present study, Wright et al. (19) also showed CD200R expression by $CD4^+$T cells and, at least at the mRNA level, preferentially by polarized Th2 cells. Thus, in Ag-specific in vivo models using reagents that modulate CD200R signaling, effects may be expected at the level of both myeloid APC and Th2 cell effector function. Enhancing inhibitory signaling received by myeloid cells may provide an overriding “off” signal to the innate and adaptive immune response and prolong graft survival or reduce autoimmune inflammation. Conversely, reagents that temporarily blockade theCD200/CD200R signaling pathway remove the dominant inhibitory effect of the inhibitory isoform of the receptor, thus promoting cellular activation and expression of NOS2 by myeloid cells. Whether Th2 cell

function is also controlled through CD200R expression is currently unknown, although the present data suggest that it may be.

What happens in the long term absence of default CD200R signaling, as occurs in the $CD200^{-/-}$ mouse? The apparently mild phenotype suggests that the CD200/CD200R axis has a specialized function that is not generally required in the normal individual. The classically activated myeloid cell phenotype, including constitutive expression of NOS2 by retinal microglia, has the short term effect of accelerating EAU disease onset, but this was not associated with increased tissue damage (20), and we now show that accelerated disease is followed by a halt in disease progress and a down-regulation of inflammation (Fig. 1). The mechanisms are not fully defined, but significantly increased numbers of $CD3^+CD4^+CD25^+$ were found in tolerized $CD200^{-/-}$ mice from day 16, with IL-10-secreting $CD11b^+$ and $CD11c^{low/-}$ cells present in the spleens of both sham-tolerized and tolerized $CD200^{-/-}$ mice from day 21 (Fig. 7). The origin and lineage of these cells are not yet understood, but because they appear 3-4 wk after disease onset, prolonged stimulation, sequential differentiation of cell subsets, and/or several rounds of cell division must be involved. Several subsets of $T_{reg}$ have been described, and although some controversy surrounds the use of particular phenotypic or cytokine secretion profiles to define them, it is clear that more than one subset of $T_{reg}$ exists and that even small numbers can have profound immunosuppressive effects (50, 59-62), either directly through inhibition of IL-2 transcription in the responder cell or indirectly through IL-10. These have been variously described as natural (typically cytokine-independent $CD4^+CD25^+$), adaptive (typically cytokine-dependent type 1 $T_{reg}$) (61), or Ag-induced (60), and there are data suggesting that several rounds of stimulation are required for the induction of adaptive $T_{reg}$ during an inflammatory response (2, 63). Although the induction of IL-10 and the suppression of IL-2 in all groups on day 28 are certainly consistent with the induction of functional $T_{reg}$ cells during the disease process (54, 55), and there are data linking nasal administration of Ag with induction of $T_{reg}1$ (36, 37), we found no direct evidence for IL-10-secreting $CD4^+$ $T_{reg}$ in spleens of protected mice.

What effect might lack of signaling through CD200R expressed by myeloid APC and Th2 cells have on mucosal tolerance induction? Significantly elevated levels of Th2 cytokines and IL-10 were prominent in the cytokine responses of tolerized CD200-deficient mice. Pulmonary DC play a critical role in the selective immune response to inhaled Ag, inducing T cell hyporesponsiveness to innocuous Ags or preferential activation and expansion of Th2-biased responses (37, 41, 42, 64). This has been attributed to the mucosal microenvironment and immature phenotype of these cells. IL-10 has also been shown to have a critical role both in the induction of nasal tolerance and in limiting inflammation later in disease (3, 34). IL-10 would then be able to augment tolerance in an Ag-specific manner, because a single exposure to IL-10 can convert DC to a tolerogenic phenotype. Examination of the draining lymph nodes and spleen of tolerized mice 24-48 h after intranasal administration of Ag revealed a pronounced induction of STAT6 expression in $CD200^{-/-}$ mice. STAT6 is required for IL-4 production (46), suggesting that an enhanced Th2 switch in response to Ag presentation could be one mechanism underlying more rapid resolution of inflammation and induction of more effective tolerance to immunizing Ag in $CD200^{-/-}$ mice. This could be due to the altered phenotype and reduced proportion of $CD11c^+$ to $CD11b^+$ RTDC present in $CD200^{-/-}$ mice presenting the nasally administered Ag in a tolerogenic fashion. However, given the endogenous state of tonic activation expected in these cells from the $CD200^{-/-}$ background, an alternative mechanism, involving active signaling, could be involved. Although Th1 responses seem to be driven by pathogen-activated innate immune responses, the signals that initiate Th2 responses are still uncertain. It has been proposed that Th2 responses emerge by default in the absence of the activating innate signals, IFN-$\gamma$ and IL-12, that would drive Th1 responses, and that alternative signals

from DC might trigger the initial production of IL-4 (56). Our data clearly show that CD200$^{-/-}$ BMDC were able to secrete equally high levels of both IL-12 and IL-10 in response to an innate maturation signal, suggesting that the cytokine bias observed in our model was induced. Because the inhibitory form of CD200R is highly expressed on polarized Th2 cells and not on Th1 cells, the inference is that the CD200/CD200R axis can regulate Th2-mediated responses.

In conclusion, we have shown that in the absence of default inhibitory CD200/CD200R signaling, accelerated EAU onset is observed in CD200$^{-/-}$ mice immunized with retinal autoantigenic peptide in CFA, consistent with an increased level of classically activated microglia and myeloid APCs in these mice. However, this response is effectively down-regulated, with significantly reduced overall disease evident at mid and late disease stages. This is consistent with induction of alternative IL-10-dependent regulatory pathways, possibly induced through dominant activating CD200RLa signaling expected in Th2 cells that are not receiving an inhibitory CD200/CD200R signal. The enhanced tolerance to EAU induction observed in CD200$^{-/-}$ mice correlated directly with up-regulated Th2-associated STAT6 activation in cervical lymph nodes of nasally tolerized mice and with elevated Th2-associated cytokine levels in response to recall Ag, again implicating active enhancement of Th2 cell activation. Additional experiments are required to confirm that dominant CD200RLa signaling preferentially activates Th2 cells in CD200$^{-/-}$ mice, leading to predominant IL-4 secretion and alternative activation of myeloid APC as a regulatory mechanism to control excessive inflammation.

## References


1. Moore KW, de Waal MR, Coffman RL, O'Garra A. Interleukin-10 and the interleukin-10 receptor. Annu. Rev. Immunol. 2001; 19:683. [PubMed: 11244051]
2. McGuirk P, McCann C, Mills KH. Pathogen-specific T regulatory 1 cells induced in the respiratory tract by a bacterial molecule that stimulates interleukin 10 production by dendritic cells: a novel strategy for evasion of protective T helper type 1 responses by *Bordetella pertussis*. J. Exp. Med. 2002; 195:221. [PubMed: 11805149]
3. Kaya Z, Dohmen KM, Wang Y, Schlichting J, Afanasyeva M, Leuschner F, Rose NR. Cutting edge: a critical role for IL-10 in induction of nasal tolerance in experimental autoimmune myocarditis. J. Immunol. 2002; 168:1552. [PubMed: 11823481]
4. Lanier LL. Face off-the interplay between activating and inhibitory immune receptors. Curr. Opin. Immunol. 2001; 13:326. [PubMed: 11406364]
5. Goerdt S, Orfanos CE. Other functions, other genes: alternative activation of antigen-presenting cells. Immunity. 1999; 10:137. [PubMed: 10072066]
6. Kuhn R, Lohler J, Rennick D, Rajewsky K, Muller W. Interleukin-10-deficient mice develop chronic enterocolitis. Cell. 1993; 75:263. [PubMed: 8402911]
7. Cant CA, Ullrich A. Signal regulation by family conspiracy. Cell. Mol. Life Sci. 2001; 58:117. [PubMed: 11229810]
8. Dietrich J, Cella M, Seiffert M, Buhring HJ, Colonna M. Cutting edge: signal-regulatory protein $\beta$1 is a DAP12-associated activating receptor expressed in myeloid cells. J. Immunol. 2000; 164:9. [PubMed: 10604985]
9. Colonna M. TREMs in the immune system and beyond. Nat. Rev. Immunol. 2003; 3:445. [PubMed: 12776204]
10. Barclay AN, Ward HA. Purification and chemical characterisation of membrane glycoproteins from rat thymocytes and brain, recognised by monoclonal antibody MRC OX 2. Eur.J. Biochem. 1982; 129:447. [PubMed: 6129975]
11. Wright GJ, Jones M, Puklavec MJ, Brown MH, Barclay AN. The unusual distribution of the neuronal/lymphoid cell surface CD200 (OX2) glycoprotein is conserved in humans. Immunology. 2001; 102:173. [PubMed: 11260322]

12. Hoek RM, Ruuls SR, Murphy CA, Wright GJ, Goddard R, Zurawski SM, Blom B, Homola ME, Streit WJ, Brown MH, et al. Down-regulation of the macrophage lineage through interaction with OX2 (CD200). Science. 2000; 290:1768. [PubMed: 11099416]
13. Gorczynski RM, Yu K, Clark D. Receptor engagement on cells expressing a ligand for the tolerance-inducing molecule OX2 induces an immunoregulatory population that inhibits alloreactivity in vitro and in vivo. J. Immunol. 2000; 165:4854. [PubMed: 11046009]
14. Gorczynski RM, Chen Z, Kai Y, Lei J. Evidence for persistent expression of OX2 as a necessary component of prolonged renal allograft survival following portal vein immunization. Clin. Immunol. 2000; 97:69. [PubMed: 10998319]
15. Barclay AN, Wright GJ, Brooke G, Brown MH. CD200 and membrane protein interactions in the control of myeloid cells. Trends Immunol. 2002; 23:285. [PubMed: 12072366]
16. Preston S, Wright GJ, Starr K, Barclay AN, Brown MH. The leukocyte/neuron cell surface antigen OX2 binds to a ligand on macrophages. Eur. J. Immunol. 1997; 27:1911. [PubMed: 9295026]
17. Wright GJ, Puklavec MJ, Willis AC, Hoek RM, Sedgwick JD, Brown MH, Barclay AN. Lymphoid/neuronal cell surface OX2 glycoprotein recognizes a novel receptor on macrophages implicated in the control of their function. Immunity. 2000; 13:233. [PubMed: 10981966]
18. Dick AD, Broderick C, Forrester JV, Wright GJ. Distribution of OX2 antigen and OX2 receptor within retina. Invest Ophthalmol. Vis. Sci. 2001; 42:170. [PubMed: 11133863]
19. Wright GJ, Cherwinski H, Foster-Cuevas M, Brooke G, Puklavec MJ, Bigler M, Song Y, Jenmalm M, Gorman D, McClanahan T, et al. Characterization of the CD200 receptor family in mice and humans and their interactions with CD200. J. Immunol. 2003; 171:3034. [PubMed: 12960329]
20. Broderick C, Hoek RM, Forrester JV, Liversidge J, Sedgwick JD, Dick AD. Constitutive retinal CD200 expression regulates resident microglia and activation state of inflammatory cells during experimental autoimmune uveoretinitis. Am. J. Pathol. 2002; 161:166. [PubMed: 12414514]
21. Dick AD. Immune mechanisms of uveitis: insights into disease pathogenesis and treatment. Int. Ophthalmol. Clin. 2000; 40:1. [PubMed: 10791254]
22. Dick AD. Immune regulation of uveoretinal inflammation. Dev. Ophthalmol. 1999; 30:187. [PubMed: 10627924]
23. Dick AD, Cheng YF, Liversidge J, Forrester JV. Immunomodulation of experimental autoimmune uveoretinitis: a model of tolerance induction with retinal antigens. Eye. 1994; 8:52. [PubMed: 8013720]
24. Dick AD, Sharma V, Liversidge J. Single dose intranasal administration of retinal autoantigen generates a rapid accumulation and cell activation in draining lymph node and spleen: implications for tolerance therapy. Br. J Ophthalmol. 2001; 85:1001. [PubMed: 11466262]
25. Jiang HR, Taylor N, Duncan L, Dick AD, Forrester JV. Total dose and frequency of administration critically affect success of nasal mucosal tolerance induction. Br. J. Ophthalmol. 2001; 85:739. [PubMed: 11371497]
26. Jiang HR, Lumsden L, Forrester JV. Macrophages and dendritic cells in IRBP-induced experimental autoimmune uveoretinitis in B10RIII mice. Invest. Ophthalmol. Vis. Sci. 1999; 40:3177. [PubMed: 10586940]
27. Dick AD, McMenamin PG, Korner H, Scallon BJ, Ghrayeb J, Forrester JV, Sedgwick JD. Inhibition of tumor necrosis factor activity minimizes target organ damage in experimental autoimmune uveoretinitis despite quantitatively normal activated T cell traffic to the retina. Eur. J. Immunol. 1996; 26:1018. [PubMed: 8647162]
28. Liversidge J, Dick A, Gordon S. Nitric oxide mediates apoptosis through formation of peroxynitrite and fas/fas-ligand interactions in experimental autoimmune uveitis. Am. J. Pathol. 2002; 160:1.
29. Gordon S. Alternative activation of macrophages. Nat. Rev. Immunol. 2003; 3:23. [PubMed: 12511873]
30. Stein M, Keshav S, Harris N, Gordon S. Interleukin 4 potently enhances murine macrophage mannose receptor activity: a marker of alternative immunologic macrophage activation. J. Exp. Med. 1992; 176:287. [PubMed: 1613462]
31. Stumpo R, Kauer M, Martin S, Kolb H. Alternative activation of macrophage by IL-10. Pathobiology. 1999; 67:245. [PubMed: 10725794]

32. Erwig LP, Kluth DC, Walsh GM, Rees AJ. Initial cytokine exposure determines function of macrophages and renders them unresponsive to other cytokines. J. Immunol. 1998; 161:1983. [PubMed: 9712070]
33. Robertson MJ, Erwig LP, Liversidge J, Forrester JV, Rees AJ, Dick AD. Retinal microenvironment controls resident and infiltrating macrophage function during uveoretinitis. Invest. Ophthalmol. Vis. Sci. 2002; 43:2250. [PubMed: 12091424]
34. Burkhart C, Liu GY, Anderton SM, Metzler B, Wraith DC. Peptide-induced T cell regulation of experimental autoimmune encephalomyelitis: a role for IL-10. Int. Immunol. 1999; 11:1625. [PubMed: 10508180]
35. Laliotou B, Duncan L, Dick AD. Intranasal administration of retinal antigens induces transient T cell activation and apoptosis within drainage lymph nodes but not spleen. J. Autoimmun. 1999; 12:145. [PubMed: 10222024]
36. Massey EJ, Sundstedt A, Day MJ, Corfield G, Anderton S, Wraith DC. Intranasal peptide-induced peripheral tolerance: the role of IL-10 in regulatory T cell function within the context of experimental autoimmune encephalomyelitis. Vet. Immunol. Immunopathol. 2002; 87:357. [PubMed: 12072259]
37. Akbari O, DeKruyff RH, Umetsu DT. Pulmonary dendritic cells producing IL-10 mediate tolerance induced by respiratory exposure to antigen. Nat. Immunol. 2001; 2:725. [PubMed: 11477409]
38. Avichezer D, Silver PB, Chan CC, Wiggert B, Caspi RR. Identification of a new epitope of human IRBP that induces autoimmune uveoretinitis in mice of the H-2b haplotype. Invest Ophthalmol. Vis. Sci. 2000; 41:127. [PubMed: 10634611]
39. Forrester JV, Huitinga I, Lumsden L, Dijkstra CD. Marrow-derived activated macrophages are required during the effector phase of experimental autoimmune uveoretinitis in rats. Curr. Eye Res. 1998; 17:426. [PubMed: 9561835]
40. Hoey S, Grabowski PS, Ralston SH, Forrester JV, Liversidge J. Nitric oxide accelerates the onset and increases the severity of experimental autoimmune uveoretinitis through an IFN-$\gamma$-dependent mechanism. J. Immunol. 1997; 159:5132. [PubMed: 9366443]
41. Stumbles PA, Thomas JA, Pimm CL, Lee PT, Venaille TJ, Proksch S, Holt PG. Resting respiratory tract dendritic cells preferentially stimulate T helper cell type 2 (Th2) responses and require obligatory cytokine signals for induction of Th1 immunity. J. Exp. Med. 1998; 188:2019. [PubMed: 9841916]
42. Prakken BJ, Roord S, van Kooten PJ, Wagenaar JP, van Eden W, Albani S, Wauben MH. Inhibition of adjuvant-induced arthritis by interleukin-10-driven regulatory cells induced via nasal administration of a peptide analog of an arthritis-related heat-shock protein 60 T cell epitope. Arthritis Rheum. 2002; 46:1937. [PubMed: 12124879]
43. Inaba K, Inaba M, Romani N, Aya H, Deguchi M, Ikehara S, Muramatsu S, Steinman RM. Generation of large numbers of dendritic cells from mouse bone marrow cultures supplemented with granulocyte/macrophage colony-stimulating factor. J. Exp. Med. 1992; 176:1693. [PubMed: 1460426]
44. Jiang HR, Muckersie E, Robertson M, Xu H, Liversidge J, Forrester JV. Secretion of interleukin-10 or interleukin-12 by LPS-activated dendritic cells is critically dependent on time of stimulus relative to initiation of purified DC culture. J. Leukocyte Biol. 2002; 72:978. [PubMed: 12429720]
45. Takeda K, Tanaka T, Shi W, Matsumoto M, Minami M, Kashiwamura S, Nakanishi K, Yoshida N, Kishimoto T, Akira S. Essential role of Stat6 in IL-4 signalling. Nature. 1996; 380:627. [PubMed: 8602263]
46. Kaplan MH, Schindler U, Smiley ST, Grusby MJ. Stat6 is required for mediating responses to IL-4 and for development of Th2 cells. Immunity. 1996; 4:313. [PubMed: 8624821]
47. Kaplan MH, Sun YL, Hoey T, Grusby MJ. Impaired IL-12 responses and enhanced development of Th2 cells in Stat4-deficient mice. Nature. 1996; 382:174. [PubMed: 8700209]
48. Thierfelder WE, van Deursen JM, Yamamoto K, Tripp RA, Sarawar SR, Carson RT, Sangster MY, Vignali DA, Doherty PC, Grosveld GC, et al. Requirement for Stat4 in interleukin-12-mediated responses of natural killer and T cells. Nature. 1996; 382:171. [PubMed: 8700208]

49. Kohm AP, Carpentier PA, Anger HA, Miller SD. Cutting edge: $CD4^+$ $CD25^+$ regulatory T cells suppress antigen-specific autoreactive immune responses and central nervous system inflammation during active experimental autoimmune encephalomyelitis. J. Immunol. 2002; 169:4712. [PubMed: 12391178]
50. Shevach EM. $CD4^+$ $CD25^+$ suppressor T cells: more questions than answers. Nat. Rev. Immunol. 2002; 2:389. [PubMed: 12093005]
51. Gorczynski RM, Chen Z, Yu K, Hu J. CD200 immunoadhesin suppresses collagen-induced arthritis in mice. Clin. Immunol. 2001; 101:328. [PubMed: 11726225]
52. Kubagawa H, Chen CC, Ho LH, Shimada TS, Gartland L, Mashburn C, Uehara T, Ravetch JV, Cooper MD. Biochemical nature and cellular distribution of the paired immunoglobulin-like receptors, PIR-A and PIR-B. J. Exp. Med. 1999; 189:309. [PubMed: 9892613]
53. Bakker AB, Wu J, Phillips JH, Lanier LL. NK cell activation: distinct stimulatory pathways counterbalancing inhibitory signals. Hum. Immunol. 2000; 61:18. [PubMed: 10658974]
54. Suri-Payer E, Amar AZ, Thornton AM, Shevach EM. $CD4^+CD25^+$ T cells inhibit both the induction and effector function of autoreactive T cells and represent a unique lineage of immunoregulatory cells. J. Immunol. 1998; 160:1212. [PubMed: 9570536]
55. Thornton AM, Shevach EM. Suppressor effector function of $CD4^+CD25^+$ immunoregulatory T cells is antigen nonspecific. J. Immunol. 2000; 164:183. [PubMed: 10605010]
56. Murphy KM, Reiner SL. The lineage decisions of helper T cells. Nat. Rev. Immunol. 2002; 2:933. [PubMed: 12461566]
57. Roncarolo MG, Bacchetta R, Bordignon C, Narula S, Levings MK. Type 1 T regulatory cells. Immunol. Rev. 2001; 182:68. [PubMed: 11722624]
58. Peiser L, Gordon S. The function of scavenger receptors expressed by macrophages and their role in the regulation of inflammation. Microbes Infect. 2001; 3:149. [PubMed: 11251301]
59. McGuirk P, Mills K. Pathogen-specific regulatory T cells provoke a shift in the Th1/Th2 paradigm in immunity to infectious diseases. Trends Immunol. 2002; 23:450. [PubMed: 12200067]
60. von Herrath MG, Harrison LC. Antigen-induced regulatory T cells in autoimmunity. Nat. Rev. Immunol. 2003; 3:223. [PubMed: 12658270]
61. Bluestone JA, Abbas AK. Natural versus adaptive regulatory T cells. Nat. Rev. Immunol. 2003; 3:253. [PubMed: 12658273]
62. Thornton AM, Shevach EM. $CD4^+CD25^+$ immunoregulatory T cells suppress polyclonal T cell activation in vitro by inhibiting interleukin 2 production. J. Exp. Med. 1998; 188:287. [PubMed: 9670041]
63. Jonuleit H, Schmitt E, Schuler G, Knop J, Enk AH. Induction of interleukin 10-producing, nonproliferating $CD4^+$ T cells with regulatory properties by repetitive stimulation with allogeneic immature human dendritic cells. J. Exp. Med. 2000; 192:1213. [PubMed: 11067871]
64. Mitchison NA, Schuhbauer D, Muller B. Natural and induced regulation of Th1/Th2 balance. Springer Semin. Immunopathol. 1999; 21:199. [PubMed: 10666769]

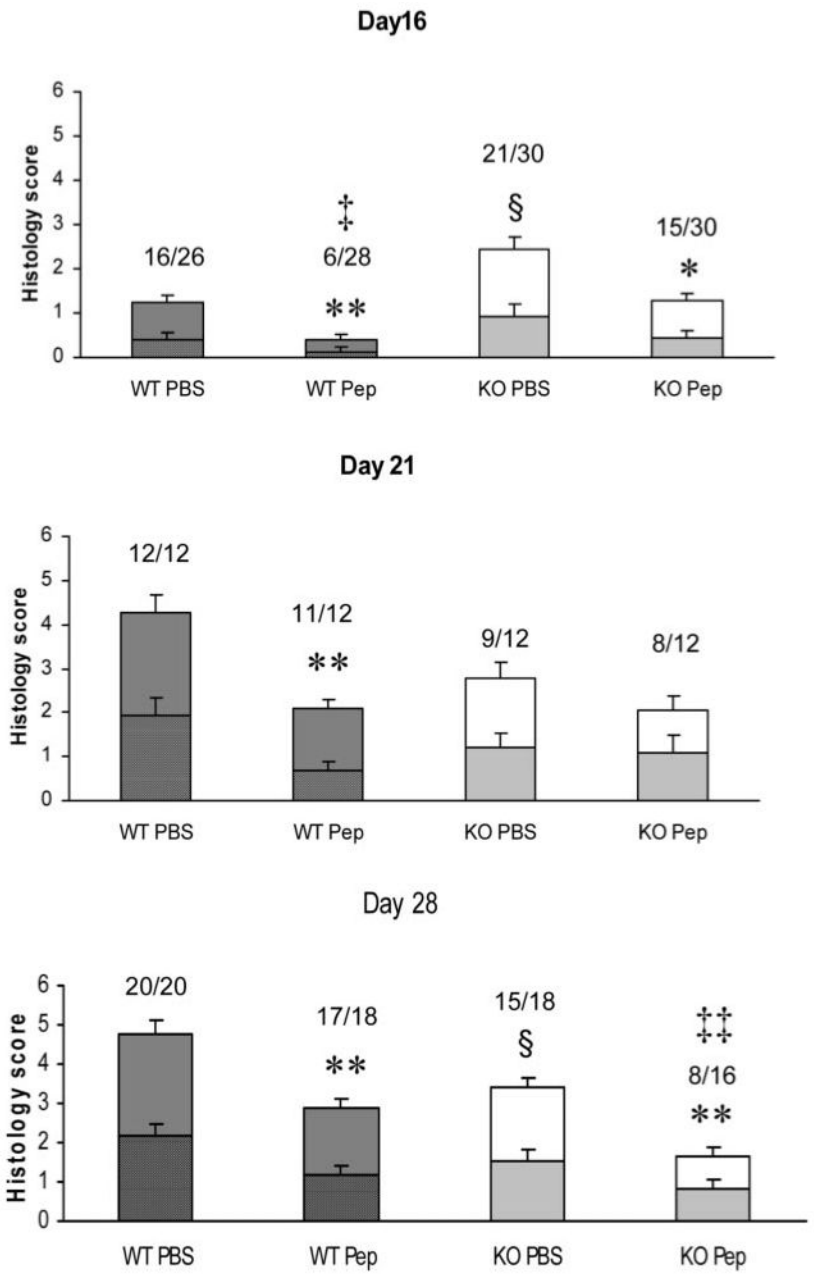


**FIGURE 1.**

Despite earlier onset of disease, tolerance induction in CD200$^{-/-}$ mice is robust, and disease is reduced over the time course compared with WT. CD200$^{-/-}$ (KO) or CD200$^{+/+}$ (WT) mice were tolerized with peptide 1-20 (Pep) or control (PBS) 10 days before immunization with peptide 1-20, and eyes were examined by resin histology or immunocytochemistry on days 16, 21, and 28 postimmunization. Histological scores were calculated and are shown as a composite bar recording inflammatory cell infiltrates (*upper bars*) and structural tissue damage (*lower bars*). Numbers above the bars indicate disease incidence in the group. Data are expressed as the mean ± SEM. Data were analyzed using the Mann-Whitney *U* test: *, $p < 0.05$; **, $p < 0.02$ (compared with sham-tolerized group); §, $p < 0.05$ (compared with WT sham-tolerized group). Significant differences in disease incidence between tolerized WT and tolerized CD200$^{-/-}$ were also found by Fisher's exact test: ‡, $p < 0.05$; ‡‡, $p < 0.006$.

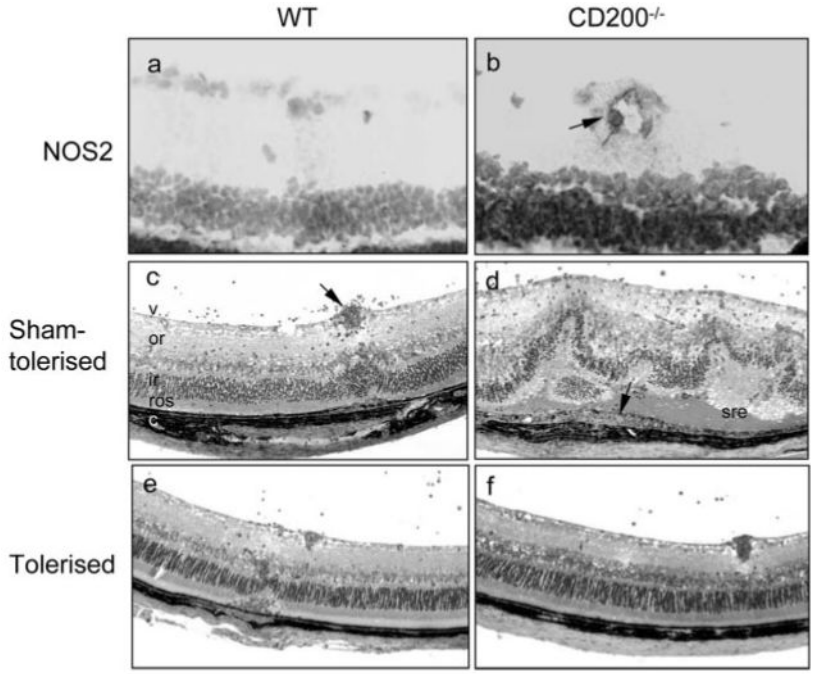


**FIGURE 2.**

Pathology of disease. Micrographs *a* and *b* are cryosections of retina from sham-tolerized mice 10 days postimmunization and stained for NOS2 showing earlier onset in CD200$^{-/-}$ mice (*b*) with an NOS2$^{+}$ leukocyte (arrowed) within a retinal vessel, the endothelium of which is also expressing NOS2. Micrographs *c*-*f* are resin histology sections from eyes 16 days postimmunization, showing more advanced disease in a sham-tolerized CD200$^{-/-}$ mouse retina (*d*) compared with WT (*c*), with significant protection in tolerized mice (*e* and *f*). Images are representative of the most severe pathology observed in each group at this time point and illustrate the main pathological features of EAU in this model. A developing focal lesion can be seen in *c*, showing cells in the vitreous (v), retinal vasculitis (arrowed) with further leukocyte infiltration of the inner retina (IR), and rod outer segments (ROS), which is the target tissue in EAU. *d*, An advanced lesion can be seen, showing extensive leukocyte infiltration and destruction of photoreceptor cells, retinal folds with a subretinal exudates (SRE), and choroidal granuloma (arrowed). In more severe cases such lesions eventually involve the whole retina. In tolerized mice significant protection is seen; inflammation is often restricted to a vasculitis with vitreous cells, with fewer cells in the inner retina, fewer retinal folds; and reduced retinal detachment. V, vitreous; or, outer retina; ir, inner retina; ros, rod outer segments; c, choroid.

Europe PMC Funders Author Manuscripts

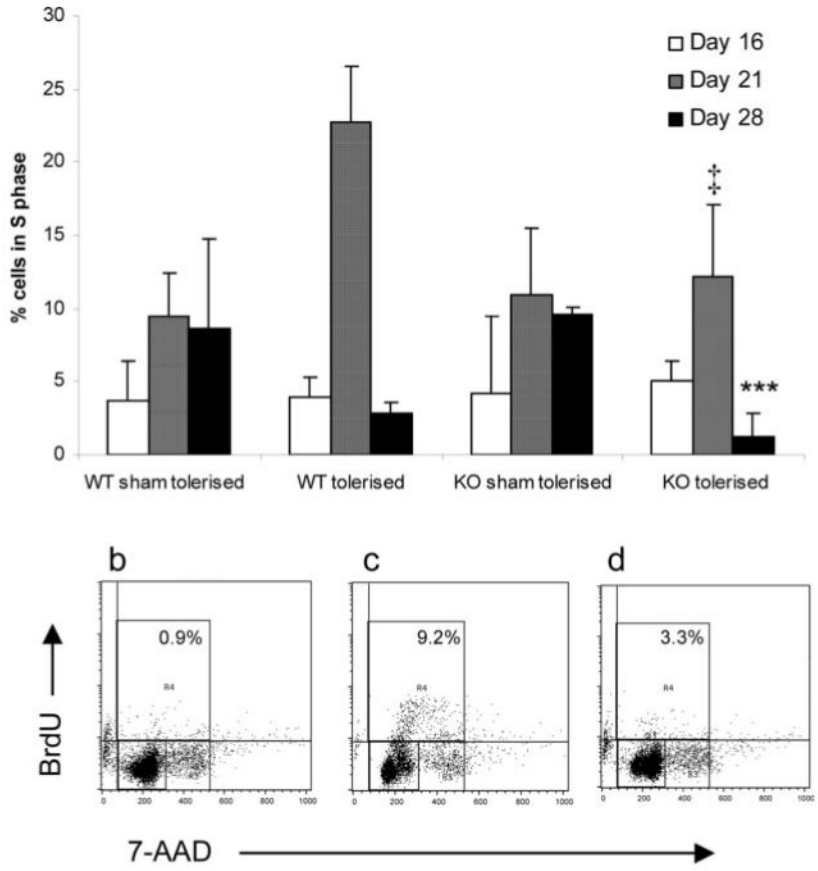


**FIGURE 3.**

Effects of tolerance induction on in vitro lymphocyte proliferation. *a*, Proliferation of splenocytes in response to stimulation with peptide 1-20 was measured by incorporation of BrdU after 96-h culture on day 16 (□), 21 (▨), and 28 (■) postimmunization with peptide 1-20. BrdU incorporation was detected by FACS analysis using an FITC-conjugated anti-BrdU Ab, and total DNA was analyzed with the dye 7-aminoactinomycin D. Proliferation in splenocytes from tolerized $CD200^{-/-}$ mice was significantly reduced compared with that in WT mice on day 21 (‡, $p < 0.02$). The overall percentage of cells in S phase was also reduced in tolerized mice on day 28, and in $CD200^{-/-}$ mice this was highly significant (***, $p < 0.001$). *b*, Representative FACS dot plot of control $CD200^{-/-}$ unstimulated culture showing the majority of cells in $G_0$-$G_1$ (R2) and 0.9% of cells in S phase (R4). *c*, Representative dot plot of stimulated splenocytes from sham-tolerized $CD200^{-/-}$ mice on day 28, showing 9.2% cells in S phase. *d*, Representative dot plot of stimulated splenocytes from tolerized $CD200^{-/-}$ mouse on day 28, showing only 3.3% cells in S phase. In all cases the majority of cells analyzed were in $G_0$-$G_1$, and no significant differences in cells progressing to $G_2$ (R3) were observed. No evidence of increased apoptosis of cells (cells in sub$G_0$) or block of cell cycle progression through $G_1$ or $G_2$ was found. Results are expressed as the mean ± 1 SD and are representative of two separate experiments.

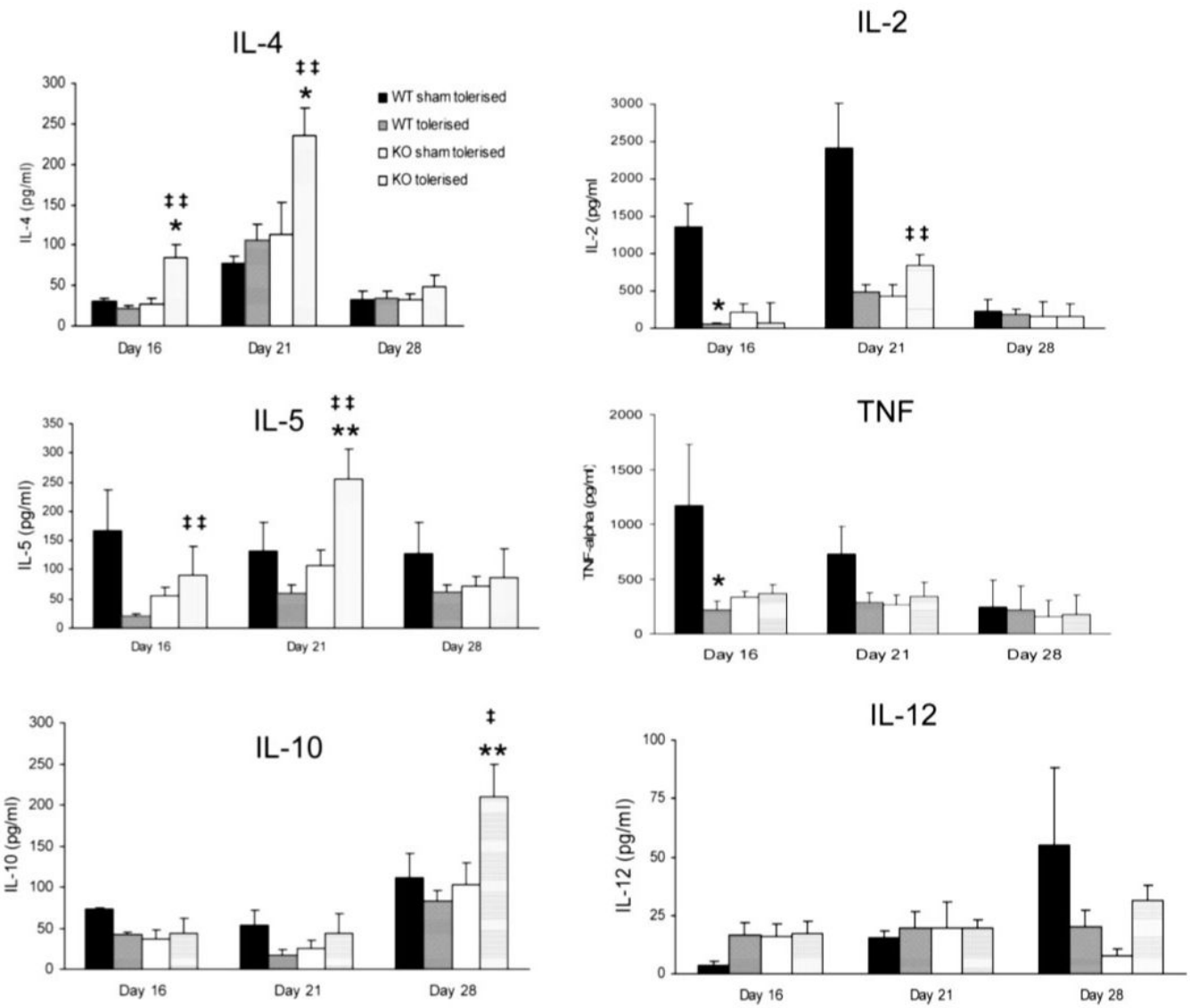


**FIGURE 4.**

Tolerance induction induces high Th2 cytokine production in CD200$^{-/-}$, but not WT, mice immunized with peptide 1-20. CD200$^{-/-}$ and WT mice were tolerized with peptide 1-20 or control PBS 10 days before immunization with peptide 1-20. Groups of at least three mice were killed on day 16, 21, or 28, and cytokine responses of splenocytes restimulated with peptide 1-20 were measured after 48 h. Cytokine data are given as picograms per milliliter and are expressed as the mean ± SEM of cumulative data from three separate experiments. *, $p < 0.05$; **, $p < 0.03$ (compared with sham-tolerized mice on same genetic background, by Mann-Whitney test). ‡, $p < 0.05$; ‡‡, $p < 0.01$ (compared with WT tolerized mice). ■, WT sham-tolerized; ▨, WT peptide-tolerized; □, CD200$^{-/-}$ sham-tolerized; ▩, CD200$^{-/-}$ peptide-tolerized.




Europe PMC Funders Author Manuscripts

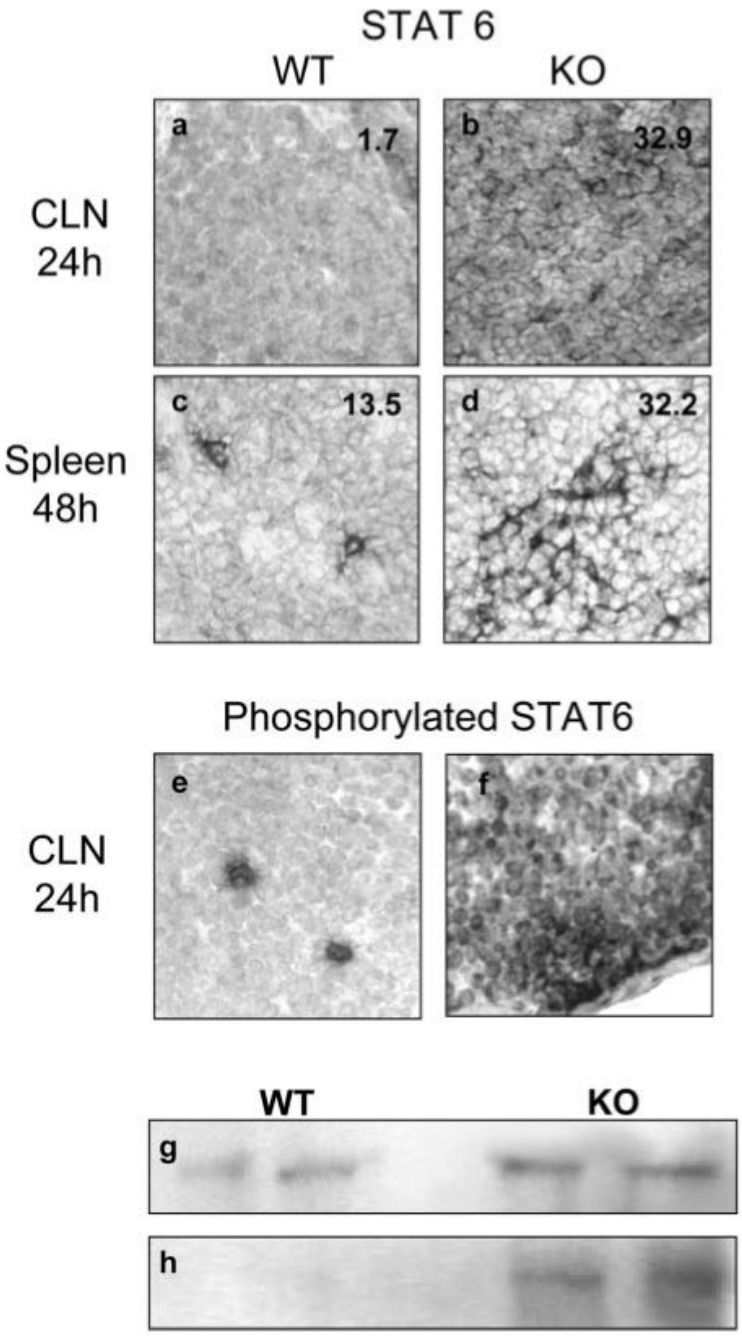


**FIGURE 5.**

STAT6 is up-regulated in draining lymph node and spleen of CD200$^{-/-}$ mice after tolerization. Sections of cervical lymph node (CLN; *a* and *b*) and spleen (*c* and *d*) were labeled with anti-STAT6 Ab using the alkaline phosphatase anti-alkaline phosphatase technique at intervals after intranasal administration of Ag, and the percentage of positively stained tissue was measured using image analysis. *a*, STAT6 WT cervical lymph node at 24 h; *b*, STAT6 knockout (KO) cervical lymph node at 24 h; *c*, STAT6 WT white pulp of spleen at 48 h; *d*, STAT6 KO white pulp of spleen at 48 h. Numbers refer to the percentage of tissue expressing STAT6 measured by image analysis. Phosphorylation of STAT6 at 24 h in cervical lymph nodes was shown by staining with a phospho-specific STAT6 mAb

(original magnification, ×40). Additional evidence of STAT6 activation was obtained by Western blotting of STAT6 immunoprecipitates from cytosolic (*g*) and nuclear (*h*) fractions of spleen leukocytes from tolerized WT and CD200$^{-/-}$ (KO) mice.



Europe PMC Funders Author Manuscripts

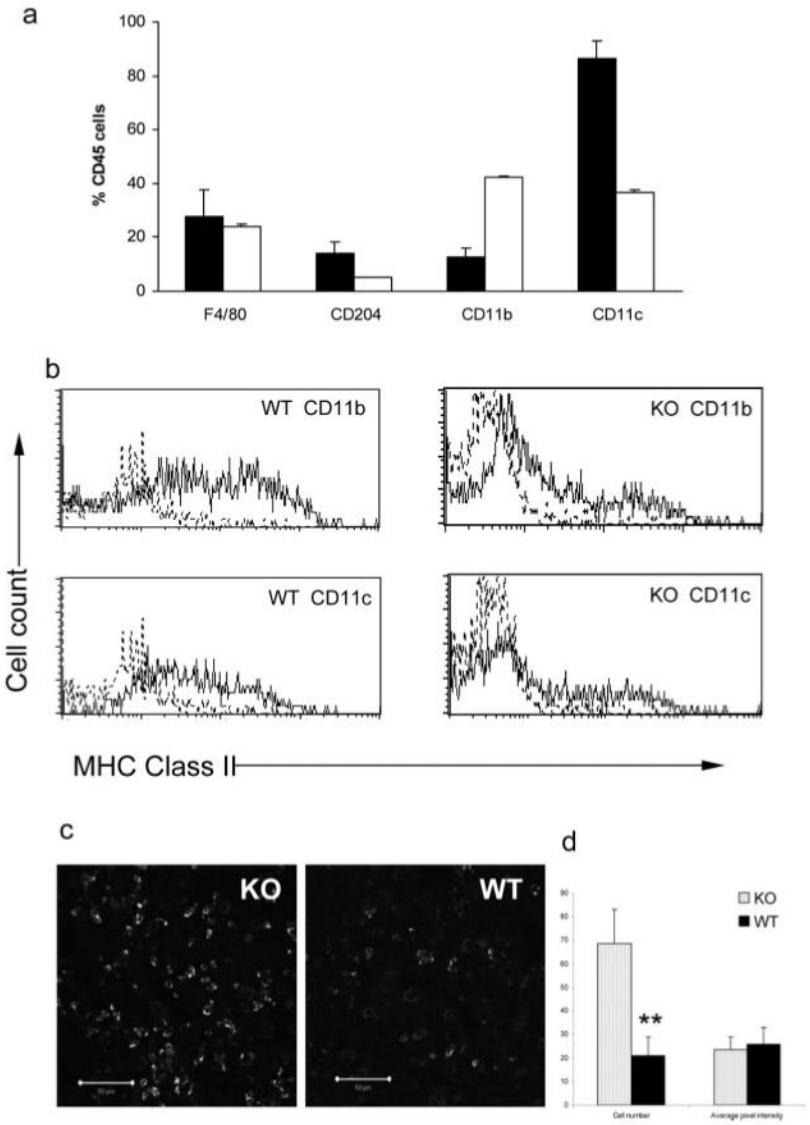


**FIGURE 6.**

Respiratory tract tissue from CD200$^{-/-}$ mice contains elevated numbers of CD11b$^{+}$ APC compared with WT tissue. Myeloid cells were purified from collagenase/DNase-treated respiratory tract tissue by density gradient centrifugation, and the phenotype of CD45$^{+}$ gated cells was analyzed by flow cytometry for the presence of CD11b$^{+}$ and CD11c$^{+}$ APC. *a*, The majority of cells from WT (■) were CD11c$^{+}$ DC. In contrast, CD200$^{-/-}$ respiratory tissue (□) contained a larger proportion of CD11b$^{+}$ cells with approximately equal percentages of CD11c$^{+}$ DC and CD11b monocytes present in the CD45$^{+}$ population. Data are expressed as the mean ± 1 SD of results pooled from two separate experiments. Values given are the percentage of positive events collected from the CD45$^{+}$ gated population. *b*, Histogram analysis of CD45 gated cells showed higher MHC class II expression by CD11b and CD11c cells in WT mice than in CD200$^{-/-}$ mice. Results are representative of four separate experiments. *c*, Confocal microscopy of frozen lung sections for CD11b expression shows that respiratory tract tissue from CD200$^{-/-}$ mice contains elevated numbers of CD11b$^{+}$ cells compared with WT tissue. *d*, Image analysis of ×20 random fields ($n$ = 24) of tissue from three WT (■) and three CD200$^{-/-}$ (□) lung samples showed a highly significant increase in

numbers of $CD11b^+$ cells per unit area in $CD200^{-/-}$ tissue. Additional analysis of fluorescence intensity showed no difference in average pixel value between the samples, indicating that levels of expression of CD11b by individual cells in the samples were equivalent. Data are shown as the mean ± SD and were analyzed using the Mann-Whitney *U* test (**, $p < 0.001$).



Europe PMC Funders Author Manuscripts

Europe PMC Funders Author Manuscripts

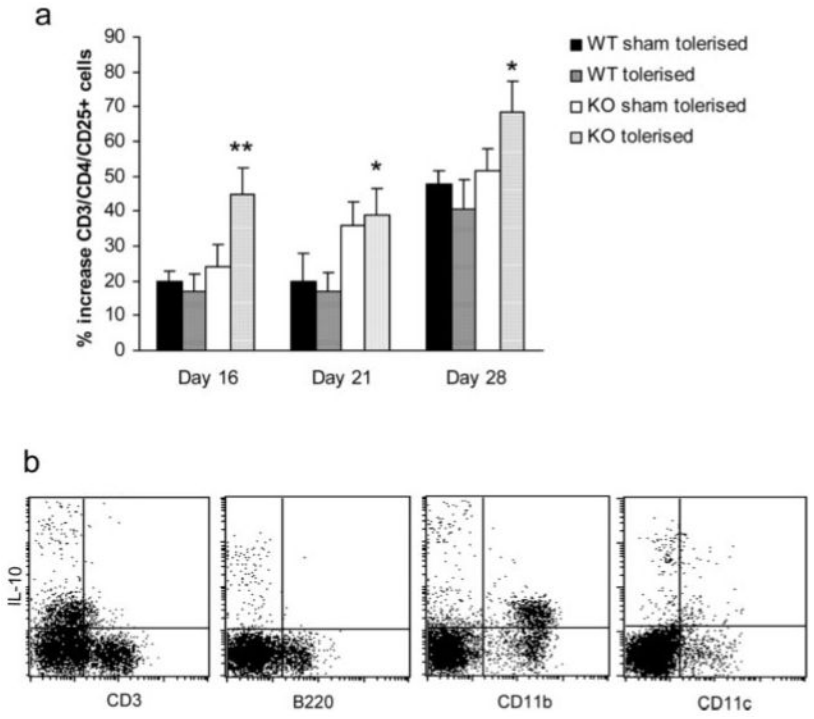


**FIGURE 7.**

Increased populations of $CD3^+CD4^+CD25^+$ T cells were present in tolerized $CD200^{-/-}$ mice. *a*, Splenocytes were analyzed by three- and four-color flow cytometry for the presence of $T_{reg}$ cells. The percentages of $CD4^+CD25^+$ T cells within the $CD3^+$ T cell population were established using three-color flow cytometry on unpermeabilized cells. A significant increase in $CD4^+CD25^+$ cells was observed in tolerized $CD200^{-/-}$ mice at all time points, and this was significant compared with that in WT tolerized mice ($p < 0.01$, by Mann-Whitney test). ■, WT sham-tolerized; ▨, WT tolerized; □, $CD200^{-/-}$ sham-tolerized; ▨, $CD200^{-/-}$ tolerized. Data are expressed as the mean ± 1 SD of at least nine animals in each group and are representative of at least three separate experiments. The percentage of $CD3^+$ cells that were $CD4^+CD25^+$ cells in normal WT mice was 8.78 ± 0.67%, and that in normal $CD200^{-/-}$ mice was 9.2 ± 2.4%. *b*, Myeloid cells express IL-10. Flow cytometric analysis of splenocytes from tolerized $CD200^{-/-}$ mice at 28 days postimmunization and direct analysis ex vivo for expression of IL-10 revealed two major populations of cells. One well-defined population with low levels of IL-10 was found to be principally $CD11b^+$ cells, and one more dispersed population that expressed much higher levels was found to be principally CD11c negative or low ($CD11c^{-/low}$). $B220^+$ cells did not express detectable levels of IL-10. A few $CD3^+$ also expressed high levels of IL-10, but these were below background (0.5% gated cells) and were not consistently observed. Data are representative of $CD200^{-/-}$ splenocyte samples from nine tolerized mice analyzed 28 days postimmunization.

Europe PMC Funders Author Manuscripts







## Table I

**Percentage of lymphoid tissue stained at time points after intranasal administration of peptide[a]**

| | CD200 WT | | | | CD200 KO | | | |
|---|---|---|---|---|---|---|---|---|
| | 0 h[b] | 4 h | 24 h | 48 h | 0 h | 4 h | 24 h | 48 h |
| Spleen red pulp | | | | | | | | |
| STAT6 | 19.0 ± 2.2 | 42.6 ± 3.7[c] | 46.6 ± 1.3[d] | 52.7 ± 4.9[c] | 25.9 ± 3.4 | 36.9 ± 5.6 | 48.5 ± 1.8[c] | 56.8 ± 4.3[c] |
| STAT4 | 19.9 ± 4.1 | 0.4 ± 0.2[c] | 5.4 ± 3.1[e] | 6.4 ± 3. | 3.4 ± 0.4[f] | 2.0 ± 0.7 | 13.6 ± 0.8[d,f] | 2.3 ± 0.3 |
| CD86 | 17.0 ± 2.9 | 32 ± 6.6 | 15.5 ± 1.8 | 18.7 ± 3.8 | 15.3 ± 2.0 | 21.3 ± 1.9 | 13.9 ± 0.9 | 26.9 ± 3.4 |
| Spleen white pulp | | | | | | | | |
| STAT6 | 3.2 ± 0.3 | 5.7 ± 1.3 | 23.5 ± 4.9[e] | 13.5 ± 2.9[e] | 3.9 ± 1.3 | 4.3 ± 0.6 | 12.81 ± 2.8[e] | 32.2 ± 4.1[c] |
| STAT4 | 5.3 ± 2.5 | 0.01 ± 0.01 | 0.4 ± 0.2 | 0.9 ± 0.3 | 0.2 ± 0.04 | 0.1 ± 0.1 | 1.5 ± 0.3[c] | 0.8 ± 0.2 |
| CD86 | 5.6 ± 0.5 | 3.2 ± 1.4 | 2.1 ± 0.7[e] | 6.1 ± 1.2 | 8.8 ± 3.9 | 3.5 ± 0.4 | 4.2 ± 1.1 | 11.8 ± 3.1 |
| Cervical lymph nodes | | | | | | | | |
| STAT6 | 6.2 ± 0.7 | 2.2 ± 1.2[e] | 1.7 ± 0.5[e] | 2.21 ± 1.6 | 6.53 ± 1.5 | 0.9 ± 0.4[e] | 32.9 ± 2.9[f,g] | 8.4 ± 1.4 |
| STAT4 | 8.0 ± 2 | 0.7 ± 0.3[e] | 0.3 ± 0.1[e] | 0.3 ± 0.15[e] | 0.4 ± 0.3[f] | 0.3 ± 0.1 | 4.0 ± 0.7[c,h] | 3.4 ± 0.8[e,f] |
| CD86 | 10.3 ± 2.4 | 14.0 ± 2.5 | 12.0 ± 3.1 | 11.0 ± 3.7 | 4.5 ± 0.6 | 4.6 ± 0.5[f] | 21.9 ± 3.6[c] | 8.1 ± 1.3 |
| Submandibular lymph nodes | | | | | | | | |
| STAT6 | 9.7 ± 3.3 | 7.6 ± 0.62 | 1.0 ± 0.51 | 1.0 ± 0.2 | 4.0 ± 1.4 | 18.8 ± 2[c,h] | 8.4 ± 2.2[f] | 12.4 ± 2[e,h] |
| STAT4 | 4.6 ± 1.2 | 1.0 ± 0.5[e] | 0.1 ± 0.04[e] | 0.03 ± 0.01[e] | 0.4 ± 0.2[f] | 0.5 ± 0.4 | 1.9 ± 0.4[h] | 0.8 ± 0.5[f] |
| CD86 | 8.7 ± 0.7 | 6.0 ± 2.5 | 3.5 ± 0.9[e] | 10.3 ± 3.3 | 1.5 ± 0.3 | 5.4 ± 0.4 | 1.8 ± 0.6 | 6.5 ± 2.5 |

[a] Data were averaged from at least three representative ×20 fields of each tissue section. Results are expressed as the mean ± SEM of data from three individual mice.

[b] Control values at 0 h taken from mice administered peptide intranasally and immediately killed. Control animals administered PBS intranasally and examined at the indicated time points showed no significant differences from 0 h values (data not shown).

[c] $p < 0.03$ vs control tissue.

[d] $p < 0.001$ vs control tissue.

[e] $p < 0.05$ vs control tissue.

[f] $p < 0.05$ vs same time in WT.

[g] $p < 0.01$ vs same time in WT.

[h] $p < 0.001$ vs same time in WT.



Europe PMC Funders Author Manuscripts